

## RELIABILITY-BASED DIAGNOSIS OF WIRELESS SENSOR NETWORK COMMUNICATION QUALITY USING READILY AVAILABLE DATA

Robin E. Kim<sup>1</sup>, Sung-Han Sim<sup>2</sup>, Kirill Mechitov<sup>3</sup>, Junho Song<sup>1</sup>, Bille F. Spencer<sup>1</sup>

<sup>1</sup>*Department of Civil and Environmental Engineering, UIUC.*

<sup>2</sup>*Department of Urban and Environmental Engineering, UNIST.*

<sup>3</sup>*Department of Computer Science, UIUC.*

### Abstract

A densely distributed wireless sensor network has the potential to provide rich information, with its low-cost and on-board computational capabilities providing significant advantage over wired sensor networks. However, communication between sensors in such networks can be challenging. Especially for wireless sensors located within civil infrastructures, which are usually made of steel and concrete, providing reliable radio communication is a key issue. Assessing network communication quality before and after finalizing a deployment is needed to achieve a robust sensor network for structural health monitoring. A framework of reliability-based diagnosis of wireless sensor network communication quality is proposed. Using radio signal strength and link quality indicators, an empirical expression for packet reception rate is derived. First-order reliability methods and Monte Carlo Simulation are further used to perform component-based reliability analyses. Predetermined information on radio signal properties enhances the applicability of the approach by requiring smaller data sets for parameter fitting. By performing the proposed analysis in complex sensor networks, an optimized sensor topology can be achieved. Moreover, periodic analyses will help with understanding the impact of temporal environmental effects on packet reception. This paper utilizes an application tool developed for the Imote2 smart sensor platform based on the Illinois Structural Health Monitoring Project Services Toolsuite.

### 1 Introduction

Developments in micro-electromechanical systems (MEMS) technology have enabled a variety of applications of smart sensors. MEMS smart sensors have greatly contributed to structural health monitoring (SHM) by offering low-cost, low-power, and low-labor demand wireless sensor networks (WSNs) to be deployed on civil infrastructures. Wirelessly collected data can be further used for system identification or damage detection of a structure and can substitute for existing wired sensor networks. Once realization of WSN for SHM is achieved, a densely distributed network is ideal for successful diagnosis of the state of the structure. Densely distributed WSNs, however, will generate a great volume of data to be wirelessly transmitted to the base station, and thus will induce not only network congestion but also high power consumption (Sim, 2011). Moreover, limited access to sensor installation sites on complex structures and budget considerations will dictate the size and topology of the network. Strength of radio transmissions between distant sensors and the base station will be adversely affected as signals are partially absorbed and reflected by the structural materials. These possible failures will result in loss of data, and Nagayama and Spencer (2007) reported that data loss will significantly degrade the accuracy of monitoring a structure. Thus, it is important to find good sensor deployment locations and to develop a protocol to ensure reliable network communication. One example of such a protocol is the general purpose reliable communication protocol developed in Illinois Structural Health Monitoring Project (ISHMP) ([www.shm.cs.illinois.edu](http://www.shm.cs.illinois.edu)) which uses multiple acknowledgments and resending of data to

mitigate data loss. However, to reduce the required number of retransmissions in order to keep network communication efficient and reduce power consumption, understanding deterministic and temporal properties of radio transmission quality is necessary.

This paper proposes a method to diagnose the state of each sensor in real time so as to account for the dynamic nature of the communication environment. Radio signal strength and link quality are assumed to vary according to determined distribution types. Structural reliability methods are adopted to assess the probability of designated events. Studied events cover the component reliability problem, which investigates failure of the event data transmission at a single node. To solve for the defined probability of events, first-order reliability methods and Monte Carlo Simulation are used, and the results verified. A practical application of network reliability is considered using the WSNs deployed on the Jindo Bridge in South Korea. The reliability assessments proposed in the paper will help with understanding the properties of data loss in a network, so that informed decisions can be made during and after deployment of wireless networks. During the deployment process, the reliability analysis can be applied to optimize sensor placement. Once the location is fixed, periodic analysis can be utilized to understand the impact of temporal environmental effects on radio signal quality, such as temperature and humidity effects or radio blockage from vehicles.

The remainder of the paper is organized as follows. In Section 2, we introduce structural reliability methods. We then develop our model and perform reliability analysis in Section 3. A campaign test to demonstrate the analysis in detail is presented in Section 4. Finally in Section 5, we apply the method to a full-scale WSN deployed on the Jindo Bridge.

## 2 Structural Reliability Methods

Structural reliability methods have been developed and applied for many applications. Structural reliability methods are applicable when random variables are continuous and their joint distributions are available. The methods are commonly used for problems requiring accurate assessment of rare events (Straub and Kiureghian, 2010).

### 2.1 First-Order Reliable Method (FORM)

In Structural Reliability Methods (SRM), failure of an event is defined as

$$F = \{g(\mathbf{x}) \leq 0\} \quad (1)$$

where  $g(\mathbf{x})$  is the limit state function consisting of basic random variable vector  $\mathbf{x}$ . When each component of vector  $\mathbf{x}$  is a continuous random variable with definable joint probability density function (PDF), then probability of an failure event  $E$  is defined in the following form (Straub and Kiureghian, 2010)

$$P_E = \int_{\mathbf{x} \in \Omega_E(\mathbf{x})} f(\mathbf{x}) d\mathbf{x} \quad (2)$$

where  $\Omega_E(\mathbf{x})$  is a set of limit-state functions. When formulating and calculating  $P_E$  requires more than one failing event, system-reliability analysis has to be considered, otherwise component reliability analysis is needed (Ditlevsen, and Madsen, 1996). We can further rewrite Equation (2) as:

$$P_E = \int_{\mathbf{x}} p_E(\mathbf{x}) f(\mathbf{x}) d\mathbf{x} \quad (3)$$

where  $p_E(\mathbf{x})$  is the conditional failure probability of failure event  $E$ . However, even for component analysis with more than two random variables, solving Equation (2) is not trivial. One of the most commonly used methods to solve it is First Order Reliable Method (Kiureghian, 2005). In FORM, transformed variables into the standard normal space ( $\mathbf{x} \rightarrow \mathbf{u}$ ) are used to obtain linearized limit-state function,

$$G(\mathbf{u}) \cong \|\nabla G(\mathbf{u}^*)\|(\beta - \alpha\mathbf{u}) \quad (4)$$

where the location of  $u^*$  is on the limit-state surface,  $G(u)=0$  with the minimum distance from the origin of the standard normal space,  $\beta$  is the reliability index, and  $\alpha$  is the normalized vector that points toward the failure domain. After linear approximation, the failure domain  $G(\mathbf{u}) \leq 0$  is redefined as  $\beta - \alpha \mathbf{u} \leq 0$ . Figure 1 summarizes the FORM approximation of the component reliability problem. In a complete form, failure probability is defined as follows

$$P_E = \Phi(-\beta) \quad (5)$$

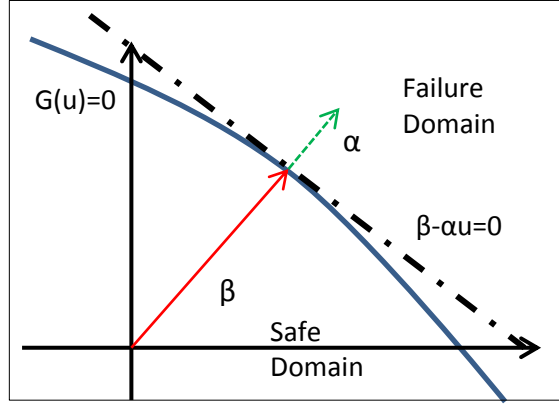


**Figure 1. FORM approximation.**

### 2.2 Monte Carlo Simulation (MCS)

The Monte Carlo method can be a powerful reliability analysis tool when a large volume of experimental data is hard to obtain. MCS introduces an indicator,  $I$ , whose value equals to 1 if the limit state function,  $g(\mathbf{x})$ , is less than zero or if the sample space lies in the failure domain and  $I = 0$  when  $g(\mathbf{x})$  is larger than zero (Ditlevsen and Madsen, 1996).

$$P_E = \int I[g(\mathbf{x}) \leq 0] f_{\mathbf{x}}(\mathbf{x}) d\mathbf{x} \quad (6)$$

Equation (6) adds  $f_{\mathbf{x}}(\mathbf{x})$  only when the state is failed, and therefore,

$$P_E = \frac{1}{N} \sum_{j=1}^N I[g(\mathbf{x}) \leq 0] \quad (7)$$

Thus, the expected value of  $P_E$  after  $N$  simulation will be

$$P_E = \frac{n_f}{N} \quad (8)$$

A large number of samples ( $N$ ) will assure accuracy of  $P_E$ . However, the computational cost of the simulation will also increase. The coefficient of variation (c.o.v.,  $\delta_{P_E}$ ) is usually realized to determine the precision of  $P_E$  and size of the sample ( $N$ )

$$\delta_{P_E} = \frac{1}{\sqrt{N}} \sqrt{\frac{1}{P_E} - 1} \quad (9)$$

For example, in order to pursue  $P_E$  to the order of  $10^{-4}$  and achieve c.o.v. to the order of 10 %, approximately  $10^4$  samples are needed in the simulation.

### 3 Prototype Problem

Consider the Imote2 wireless smart sensor from MEMSIC (Figure 2, a) and the ISM400 sensor board (Figure 2, b) developed at the University of Illinois at Urbana-Champaign. A 2.4 GHz SMD external

antenna is attached to each Imote2. The Illinois Structural Health Monitoring Project Services Toolsuite is used for the supporting software for the wireless sensor platform ([www.shm.cs.illinois.edu](http://www.shm.cs.illinois.edu)).



**Figure 2. (a) Imote2 and (b) ISM400 sensor board.**

The TestRadio utility in the ISHMP Toolsuite assesses the communication status between a base station (sender) and leaf nodes (receivers) by calculating the fraction of packets received and radio signal strength values. An example of TestRadio output for a base station that attempted to send 1000 round-trip packets to a leaf node (node ID: 53) is shown in Figure 3. Returned Radio Signal Strength Indicator (rRSSI) and returned Link Quality Indicator (rLQI), both measured by the radio hardware, are further used to represent the signal environment status at the leaf nodes.

```

BluSH>TestRadio 1000 53
BluSH>Sending 1000 packets to 1 node(s): 53
Request successfully sent to 1 node(s).
Sending data messages...
Data messages sent.
Querying node 53...
Finished receiving responses from node 53.
addr  cnt  %  rssi  lqi  rcnt  r%  rrsi  rlqi
se
53    1000  100  -37   106  1000  100  -36   107

```

**Figure 3. TestRadio utility example.**

### 3.1 Distribution Model and Joint PDF of Random Variables

An extensive indoor measurement using TestRadio was conducted to find the distribution of two random variables, RSSI and LQI. In each test, 100 packets were sent out to single or multiple leaf nodes. On receiving the packets, the leaf nodes resent the packets back to the base station, with information about RSSI and LQI. Packet Reception Rate (PRR), which is the ratio between received and sent packets, is taken as the measure of data loss. At a fixed location, 5 m away from the base station, the 100-packet TestRadio test was performed 500 times. In order to reduce hardware related bias, three different Imote2s were used.

**Table 1. TestRadio setup.**

Number of Imote2s used	3
Distance to leaf nodes (m)	5
Packets sent in each trial	100
Number of trials	500

Then, PDFs of the random variables were modeled. The distribution models were selected using ‘difttool’ in Matlab®, with the maximum likelihood estimation method. While selecting the appropriate models for the PDF, the criteria were:

1. The shape of the selected PDF of a random variable should well represent that of the histogram.
2. The boundary of each distribution should not violate physical limitations of random variables.

Suggested PDF for RSSI is the normal distribution with mean value ( $\mu_{\text{RSSI}}$ ) of -92.60 dB and standard deviation ( $\sigma_{\text{RSSI}}$ ) of 1.43. A Gamma distribution is suggested for LQI, with the following parameters:  $\mu_{\text{LQI}}= 97.50$ ,  $\sigma_{\text{LQI}}= 36.24$ ,  $a_{\text{LQI}}= 262.335$  and  $b_{\text{LQI}}= 8.6 \times 10^{-4}$  (Figure 4). The measured RSSI data is a quantized integer value, and thus the histogram shows a discontinuity between integers, compared to the continuous PDF. Important to note is that the mean and variance of RSSI and LQI models can change with the environmental effects such as the distance from the base station or structural obstructions. Whereas the distribution types, normal distribution for RSSI and Gamma distribution for LQI, are less likely to be changed, since hardware related biases are accounted for by using different Imote2s for each test and were combined to find the distribution models. Thus, in further applications, smaller amounts of data, only enough to find the parameters fitting for determined distribution types, is needed. This approach enhances the applicability of the method for analyzing in-place wireless sensors.

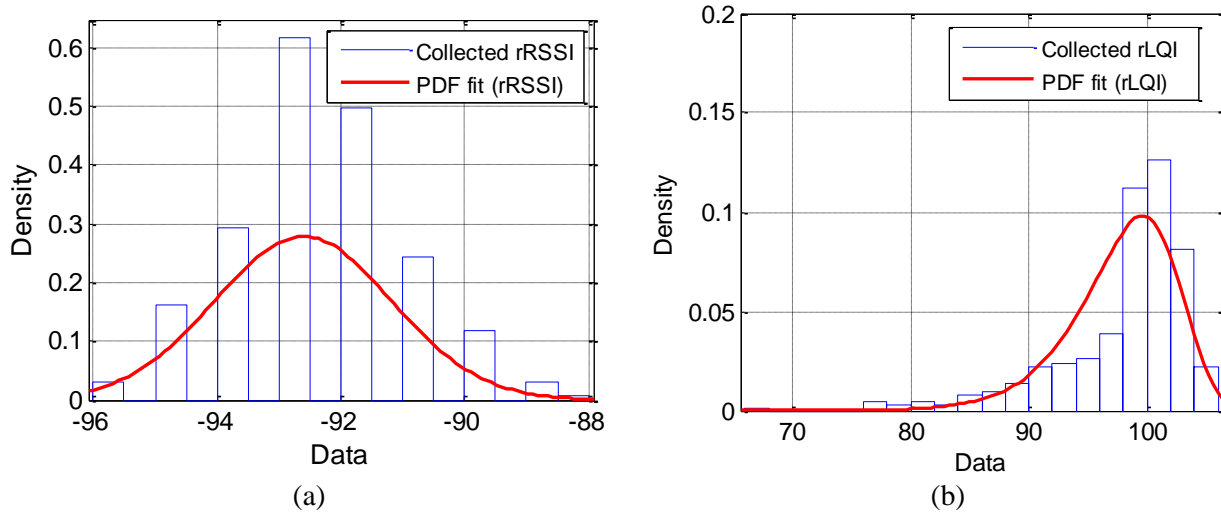


**Figure 4. Histograms and suggested PDFs for (a) RSSI and (b) LQI.**

According to Equation (2), for any limit state function, identifying the joint PDF and standardized joint normal PDF is important for further analysis. The Nataf distribution model is used to transfer a joint PDF model of RSSI and LQI (Figure 5). Correlation coefficient ( $\rho_{ij}$ ) between transformed random variables ( $z_i, z_j$ ) is defined as shown in Equation (10)

$$\rho_{ij} = \int_{-\infty}^{\infty} \int_{-\infty}^{\infty} \left( \frac{x_i - \mu_i}{\sigma_i} \right) \left( \frac{x_j - \mu_j}{\sigma_j} \right) \varphi_2(z_i, z_j, \rho_{0,ij}) dz_i dz_j \quad (10)$$

where  $z_i$  and  $z_j$  are random variables in the transformed domain,  $\rho_{0,ij}$  is the correlation coefficient of random variables  $x_i$  and  $x_j$ , and  $\varphi_2$  is the bivariate standard normal PDF (Liu and Kiureghian, 1986).

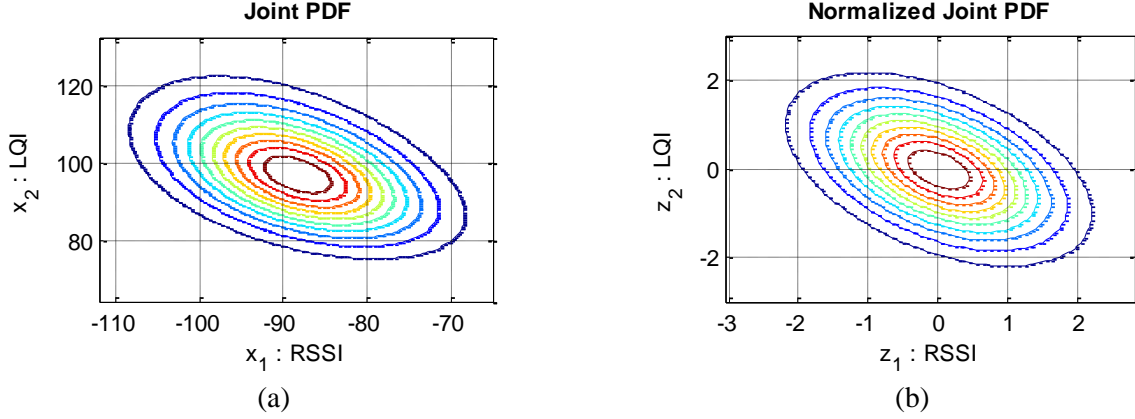


**Figure 5. (a) Joint PDF of RSSI and LQI and (b) Normalized joint PDF.**

### 3.2 Limit State Function

Failure of a leaf node in this study is defined as the amount of data loss, as determined by the PRR. If successfully returned packets are less than 85 % of attempted packets sent,  $g(x) \leq 0$ , the leaf node is assumed to have a harsh radio communication environment, which also results in low RSSI and LQI values.

$$g(x) = \text{PRR}(\text{RSSI}, \text{LQI}) - \text{Threshold}(\text{PRR} \leq 85\%) + \text{error}(\varepsilon) \quad (11)$$

$$\begin{aligned} g(x) &\leq 0 && \text{failure set} \\ g(x) &= 0 && \text{limit state surface} \\ g(x) &> 0 && \text{safe set} \end{aligned}$$

In order to find an expression of  $\text{PRR}(\text{RSSI}, \text{LQI})$  in Equation (11), the RSSI, LQI, and PRR measurements collected from the test setup defined in Table 1 are explored (Figure 6). The relationship shows an overturned ‘L-shape’, which starts at RSSI value of -85 dB and 90 LQI. As RSSI and LQI values decrease, packet reception rate decreases dramatically. The PRR is more sensitive to changes in LQI than changes in RSSI with correlation coefficient being  $\rho_{\text{LQI}, \text{PRR}} = 0.80$ , while  $\rho_{\text{RSSI}, \text{PRR}} = 0.49$ .

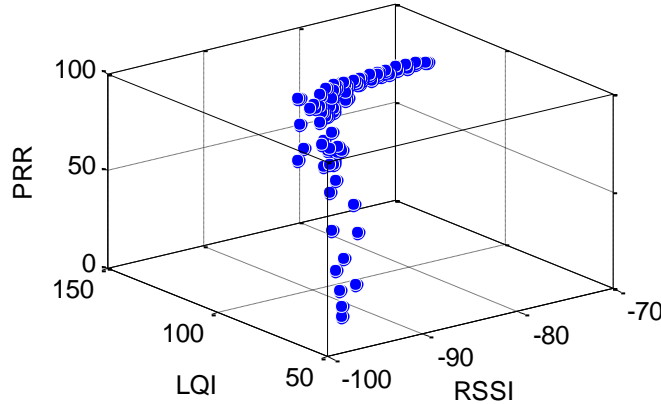


**Figure 6. RSSI, LQI and PRR relationship.**

Using ‘sftool’ in Matlab<sup>®</sup>, a second order polynomial model was obtained with  $R^2 = 0.87$  (Figure 7).

$$\text{PRR}_{\text{est}} = a + b * \text{RSSI} + c * \text{LQI} + d * \text{RSSI}^2 + e * \text{RSSI} * \text{LQI} + f * \text{LQI}^2 \quad (12)$$

$$\begin{aligned} \text{where, } a &= -4434, & b &= -42.75, \\ c &= 54.51, & d &= -0.1319, \end{aligned}$$

$$e = 0.2053, \quad f = -0.1851.$$

The correlation coefficients  $\rho_{LQI,PRR}$  and  $\rho_{RSSI,PRR}$  both slightly increased in  $PRR_{est}$  which is calculated with the fitted model ( $\rho'_{LQI,PRR_{est}} = 0.86$  and  $\rho'_{RSSI,PRR_{est}} = 0.52$ ).

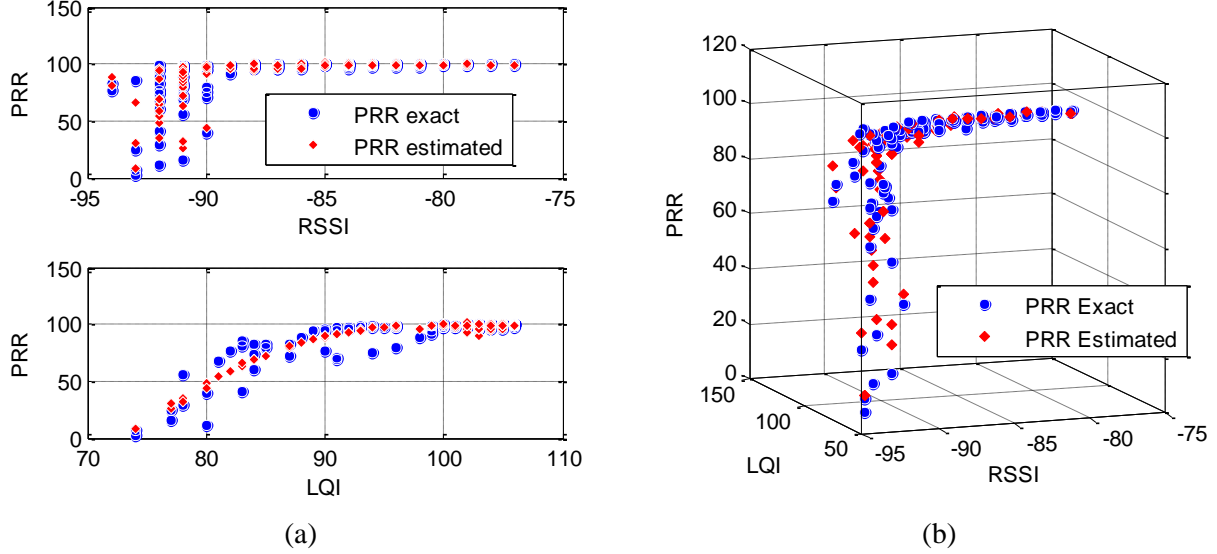


**Figure 7. Estimated PRR value with fitted model (a) RSSI-PRR; top, LQI-PRR; bottom, (b) RSSI-LQI-PRR relationship.**

In order to compensate for the epistemic error as shown in Figure 7, an error term ( $\varepsilon$ ) is introduced in Equation (12). With the Central Limit Theorem, a distribution model of  $\varepsilon$  is assumed to follow the normal distribution with zero mean and standard deviation  $\sigma$ , determined during regression analysis  $\varepsilon(RSSI, LQI) \sim N(0, \sigma)$ . A linear regression method is used to find an unbiased estimation of the conditional variance of  $\varepsilon$  for given values of RSSI and LQI (Straub and Kiureghian, 2010).

## 4 Reliability Analysis on a Campaign Test

### 4.1 FORM Analysis

So far, we have defined distribution types of random variables (RSSI, LQI, and epistemic error), Joint PDF of RSSI and LQI and limit state function  $g(x)$ . For further reliability analysis, outdoor TestRadio at 3 different locations (15 m, 30 m and 45 m from the base station) were conducted. At each location, 3 Imote2s were used to mitigate hardware related bias. By considering the RSSI and LQI values sent by the Imote2s and the corresponding packet loss information to represent the location of the Imote2s, component reliability analyses are selected. A total of 100 TestRadio trials were performed, and at each TestRadio trial, 100 packets were transmitted. Table 2 summarizes the FORM analyses result for each test setup using Matlab-based reliability software, FERUM developed at University of California, Berkeley (Kiureghian, *et al.*, 2006).

**Table 2 TestRadio setup for campaign test.**

	Location from Base Station	$P_E$	$\beta$	Failure point	
				RSSI	LQI
Test Setup 1	15 m	0.0584	1.5681	-77.25 dB	106.16
Test Setup 2	30 m	0.1182	1.1838	-82.35 dB	102.20
Test Setup 3	45 m	0.1772	0.9262	-82.16 dB	99.78

$P_E$  denotes the failure probability and  $\beta$  is the reliability index, as shown in Equation (5). The geometric meaning of  $\beta$  is defined as the distance in the normalized space from the origin to the limit state surface (Ditlevsen and Madsen, 1996) The last two columns denote the nearest failure RSSI and LQI pairs from origin on the limit state surface. Although  $P_E$  increases with distance from the base station,  $P_E$  for all the cases are as small as 0.1772, indicating that communication between Imote2s is robust within a distance of 50 m.

#### 4.2 MCS Analysis

The failure probabilities for Test Setup 1, 2 and 3 (Table2) are computed also using Monte Carlo Simulation (MCS). Although MCS is less efficient in computational requirements than FORM analyses, MCS is a powerful computational tool that can generate large dimensional data with highly faithful and accurate sampling (Kang *et al.*, 2009). The validity of MCS is checked by its coefficient of variation (c.o.v.). Converging c.o.v. with a small value indicates that the sufficient number of samples to validate the MCS is generated. For example, Figure 8 shows the converging trend of failure probability ( $P_E$ ) and c.o.v. for Test Setup 1 (Table 2) as number of sampling increases to  $10^4$ . c.o.v. converged agreeably at  $10^4$  samples, validating the failure probability result at  $P_E(10^4)$ .

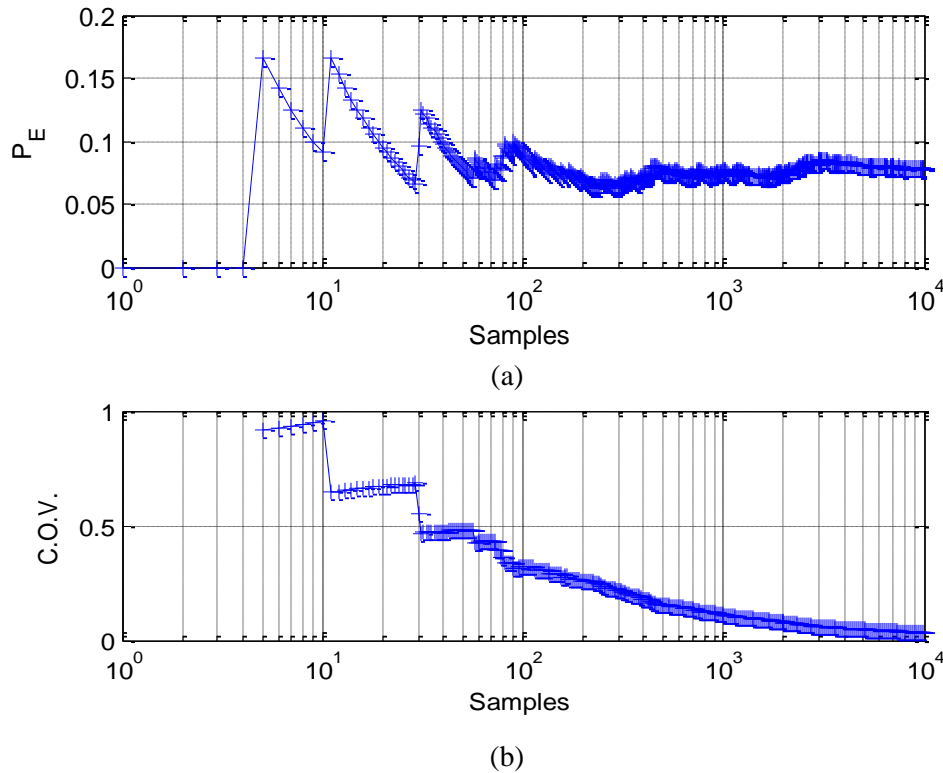


**Figure 8. MCS result: (a) Probability of failure and (b) c.o.v.**

Table 3 summarizes  $P_E$  obtained from MCS ( $10^4$  samples) and compares it with that of FORM. As distance from the base station increases, probability of failure gradually increases both in MCS and FORM. However, MCS results are larger than FORM with roughly a 40% difference. These differences indicate that FORM analysis yields a less conservative result than MCS. Also, with distributions, correlation coefficients of random variables, and the limit-state function identified, MCS analysis can provide a better result by using a large number of samples.

**Table 3 MCS results and comparison with FORM results.**

	Location from Base Station	FORM	MCS	Error [ % ]
		$P_E$	$P_E$	
Test Setup 1	15 m	0.0584	0.0771	24.25 %
Test Setup 2	30 m	0.1182	0.2013	41.28 %
Test Setup 3	45 m	0.1772	0.2855	37.93 %

## 5 Reliability Analysis on a Full-Scale WSSN on the Jindo Bridge

ISHMP deployed a full-scale WSN in Jindo Bridge, Jindo, South Korea. In the latest deployment, 113 sensors nodes (669 channels in total) have been installed. Span length is 344 m for main span and 70 m for each side spans. Due to the size of the network, the WSSN is divided into 4 sub-networks; Jindo side 1) deck network, 2) cable network, Haenam side 3) deck network and 4) cable network. Also, to enhance the communication, an 8 dBi antenna with a noise compensator is used for each deck base station gateway node. Figure 9 shows the deployment map for the entire WSSN. The scope of this study covers selected 12 nodes in Haenam deck nodes (Figure 9, (b)). The location of the base station for this network was on Haenam side's pylon pier. Thus, maximum distance from a leaf node to the base station is approximately 170 m for node Id 113 and 151.

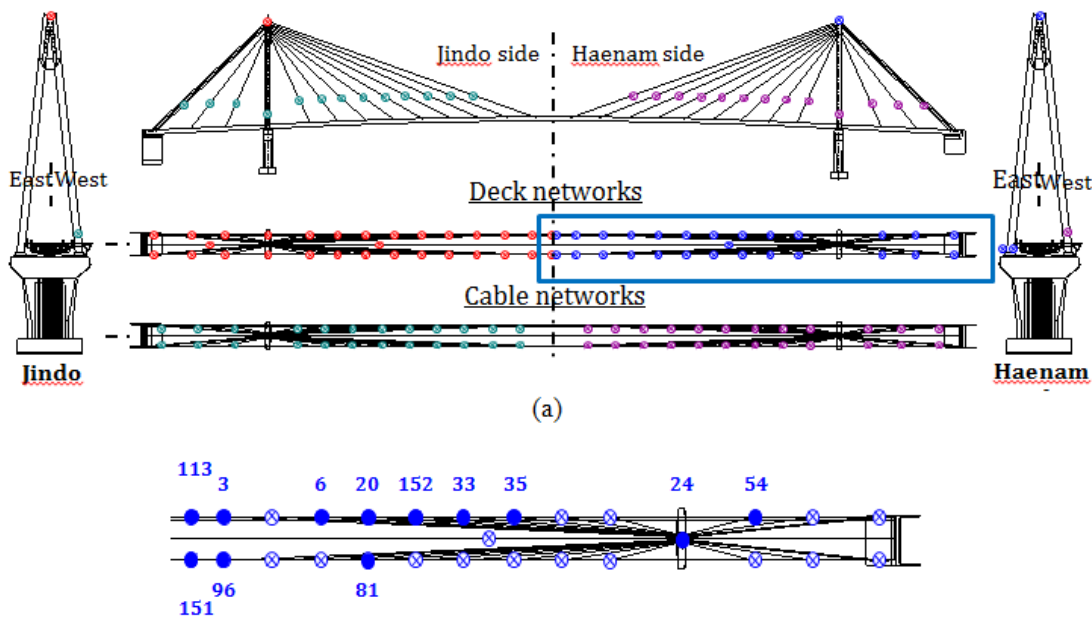


**Figure 9. (a) Sensor topology for Jindo Bridge and (b) Sensors utilized for MCS.**

Approximately 100 TestRadio trials sending 100 packets for each attempt were conducted to collect RSSI, LQI and PRR measurements. MCS with  $10^4$  samples is found more appropriate over FORM for component analysis of the Jindo WSN. Table 4 summarizes the probability of failure at selected nodes. With converging c.o.v.,  $P_E$  values were found to be very small, except for node Id 3. The conclusion drawn here is that with the help of extra antenna devices installed, communication at Jindo Bridge is very robust to cover entire range of a subnetwork.

**Table 4. MCS results using Haenam deck nodes.**

Node Id	c.o.v.	$P_E$	Node Id	c.o.v.	$P_E$
<b>54</b>	0.0863	0.0013	<b>81</b>	0.0478	0.0043

<b>24</b>	0.0180	0.0298	<b>6</b>	0.0596	0.0028
<b>35</b>	0.0460	0.0047	<b>3</b>	0.0048	0.3059
<b>33</b>	0.0448	0.0050	<b>96</b>	0.0354	0.0001
<b>152</b>	0.0406	0.0060	<b>113</b>	0.0510	0.0010
<b>20</b>	0.0415	0.0058	<b>151</b>	0.0333	0.0001

## 6 Conclusions

Component-based reliability analysis of wireless sensor network data loss has been proposed in the study. Using readily available data, RSSI and LQI measurements, FORM and MCS analysis to assess the failure probability ( $P_E$ ) of packet reception is calculated and compared. The proposed method utilizes predetermined distribution types for RSSI and LQI, enhancing the applicability by requiring a smaller data set. In a campaign test, FORM result yields a smaller value than that of MCS result, in which larger  $P_E$  shows a conservative approach. MCS has been also applied to assess the radio communication reliability of the full scale deployment on Jindo Bridge, Korea. Due to the strengthened radio power with extra Antenna devices, the Jindo WSN showed robust radio communication over the entire sub-network. Reliability analysis before a long-term deployment is thus beneficial to assuring the communication capabilities of the wireless sensors. Depending on the degree of radio quality needed, not only the distance between to a leaf node but also radio power and antenna devices can be determined. Periodic assessment is also required to understand in-place radio quality, which can be affected by temporal changes in the environment. In complex networks, particularly when data loss is affected by structures/environment, early inspection of radio quality along with periodic assessment will lead further to successful long-term structural monitoring using WSNs.

## References

- Sim. S. (2011). "Decentralized Identification and Multimetric Monitoring of Civil Infrastructure Using Smart Sensors." *Ph. D. dissertation, University of Illinois at Urbana-Champaign.*
- Nagayama T., and Spencer B. F. (2007). "Structural Health Monitoring Using Smart Sensors." *Newmark Structural Engineering Laboratory Report Series*, No. 001.
- ISHMP website, [www.shm.cs.illinois.edu](http://www.shm.cs.illinois.edu).
- Straub D., and Kiureghian A. D. (2010). "Bayesian Network Enhanced with Structural Reliability Methods: Methodology." *Journal of Engineering Mechanics*, 136 (10), 1248 - 1258.
- Ditlevsen O., and Madsen H. O. (1996). "Structural Reliability Methods." *J. Wiley & Sons.*
- Kiureghian A. D. (2005). "First- and second-order Reliability Methods," *Engineering design reliability handbook.*
- Liu P. L., and Kiureghian A. D. (1986). "Multivariate Distribution Models with Prescribed Marginals and Covariances." *Probabilistic Engineering Mechanics*, 1(2), 105–12.
- Kiureghian A. D., Haukaas T., and Fujimura K. (2006). "Structural Reliability Software at the University of California, Berkeley." *Journal of Structural Safety*, 28 (1), 44-67.
- Kang W.H., Lee Y. J., Song J., and Gencturk B. (2009). "Further Development of Matrix-based System Reliability Method and Applications to Structural Systems." *Structure and Infrastructure Engineering.*